analytical chemistry

Article

Cite This: *Anal. Chem.* 2018, 90, 14610−14615

pubs.acs.org/ac

Direct Quantitative Analysis of Multiple microRNAs (DQAMmiR) with Peptide Nucleic Acid Hybridization Probes

Liang Hu,[†] Mansi Anand,[†] Svetlana M. Krylova,[†] Burton B. Yang,[‡] Stanley K. Liu,[§] George M. Yousef,[∥] and Sergey N. Krylov*[,†]

[†]Department of Chemistry and Centre for Research on Biomolecular Interactions, York University, Toronto, Ontario M3J 1P3, Canada

[‡]Sunnybrook Research Institute and Department of Laboratory Medicine and Pathobiology, Faculty of Medicine, University of Toronto, Toronto, Ontario M5S 1A8, Canada

[§]Department of Radiation Oncology, Sunnybrook-Odette Cancer Centre, 2075 Bayview Avenue, Toronto, Ontario M4N 3M5, Canada

[∥]Keenan Research Centre, St. Michael's Hospital, 30 Bond Street, Toronto, Ontario M5B 1W8, Canada

Supporting Information

ABSTRACT: Direct quantitative analysis of multiple miRNAs (DQAMmiR) is a hybridization-based assay, in which the excess of the DNA hybridization probes is separated from the miRNA-probe hybrids, and the hybrids are separated from each other in gel-free capillary electrophoresis (CE) using two types of mobility shifters: single-strand DNA binding protein (SSB) added to the CE running buffer and peptide drag tags conjugated with the probes. Here we introduce the second-generation DQAMmiR, which utilizes peptide nucleic acid (PNA) rather than DNA hybridization probes and requires no SSB in the CE running buffer. PNA probes are electrically neutral, while PNA−miRNA hybrids are negatively charged, and this difference in charge can be a basis for separation of the hybrids from the probes. In this proof-of-principle work, we first experimentally confirmed that the PNA−RNA hybrid was separable from the excess of the PNA probe without SSB in the running buffer, resulting in a near 10 min time window, which would allow, theoretically, separation of up to 30 hybrids. Then, we adapted to PNA−RNA hybrids our previously developed theoretical model for predicting hybrid mobilities. The calculation performed with the modified theoretical model indicated that PNA−RNA hybrids of slightly different lengths could be separated from each other without drag tags. Accordingly, we designed a simple experimental model capable of confirming: (i) separation of tag-free hybrids of different lengths and (ii) separation of same-length hybrids due to a drag tag on the PNA probe. The experimental model included three miRNAs: 20-nt miR-147a, 20-nt miR-378g, and 22-nt miR-21. The three complementary PNA probes had lengths matching those of the corresponding target miRNAs. The probe for miR-147a had a short five-amino-acid drag tag; the other two had no drag tags. We were able to achieve baseline separation of the three hybrids from each other. The LOQ of 14 pM along with the high accuracy (recovery >90%) and precision (RSD ≈ 10%) of the assay at picomolar target concentrations suggest that PNA-facilitated DQAMmiR could potentially support practical miRNA analysis of clinical samples.

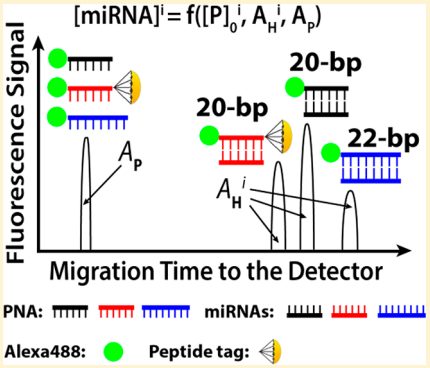

MicroRNAs (miRNAs) are short single-strand RNA molecules (18−25 nucleotides) that play key roles in fundamental cellular processes such as cell differentiation, proliferation, and apoptosis.[1,2] Aberrant miRNA expression affects these processes and, as a result, leads to various pathological outcomes. In particular, abnormal miRNA expression has been linked with Alzheimer's disease, heart diseases, and multiple cancers.[3−5] For example, abnormal expression of groups of 2, 3, and 4 miRNAs were found to be indicative of prostate, lung, and breast cancers in humans.[6−8] Clinical use of reliable miRNA-based disease biomarkers requires accurate and robust quantitative analyses of multiple miRNAs in clinical samples.

Many existing methods of miRNA detection, including microarray-based techniques, quantitative reverse transcription polymerization chain reaction, and next-generation sequencing, are indirect, i.e., they require modification or amplification of miRNA targets. Such manipulations with the targets introduce sequence-related biases in the analyses.[9,10] Other techniques have also been developed for direct quantitation of multiple miRNAs, such as mass spectrometry,[11,12] electrochemical sensing,[13,14] optical resonance,[15] and etc.[16−19] However, methods based on these techniques often require isolation of

Received: October 18, 2018
Accepted: November 19, 2018
Published: November 19, 2018

DOI: 10.1021/acs.analchem.8b04793
Anal. Chem. 2018, 90, 14610−14615

total RNA from the sample before measuring miRNA; such sample processing involves a time-consuming purification step and introduces analytical inaccuracies.[20,21] There are very few methods that can satisfy the criteria of direct quantitation of multiple miRNAs with minimal sample processing.[13,17] One of such approaches is direct quantitative analysis of multiple miRNAs (DQAMmiR) by gel-free capillary electrophoresis (CE),[22] which has been proven to be robust in analyzing miRNAs in crude cell lysate.[23] In general, DQAMmiR is a hybridization-based assay, in which the excess of hybridization probes (fluorescently labeled for sensitive detection) is separated from the miRNA-probe hybrids, and the hybrids are separated from each other, by CE with strong electroosmotic flow (EOF). The EOF propels the probes and the hybrids toward the detector at the end of the capillary; quantitative detection of the probes and the hybrids facilitates absolute quantitation of the hybrids without calibration curves.

The first generation of DQAMmiR utilizes ssDNA probes and two types of mobility shifters: (i) ssDNA binding protein (SSB) added to the running buffer[24] and (ii) different-length-peptide drag tags conjugated onto the ssDNA probes.[25] SSB facilitates separation of the excess probes from the hybrids by binding the ssDNA probes but not the hybrids. The drag tags induce mobility shifts in the hybrids, allowing their separation from each other without interference with the binding affinity of SSB to the ssDNA probes. However, SSB is a protein, and while it is quite stable, involving it in the assay can potentially decrease the assay's robustness and increase its cost, making it less suitable for practical clinical use.

To address this issue, here, we introduce the second-generation DQAMmiR, which does not need SSB and has lesser dependence on drag tags on the probes. The function of SSB, utilized in the first-generation DQAMmiR, is to separate the excess ssDNA probes from the ssDNA−miRNA hybrids, which have similar electrophoretic mobilities due to negative charges on both DNA and RNA. SSB would not be needed if the probes were polymers capable of hybridizing miRNA but not being negatively charged. An example of such polymers is peptide nucleic acid (PNA), which is an electrically neutral analogue of DNA composed of repeating *N*-(2-amino-ethyl)-glycine units.[26] PNA−miRNA hybrids are negatively charged due to the negative charge on miRNA, although the charge density is about half of that of DNA−miRNA hybrids. Electrically neutral PNA probes should be separable from the negatively charged PNA−miRNA hybrids without any additional mobility modifier, such as SSB.

To achieve quantitation of multiple targets, separating the hybrids from each other is also essential. A theoretical model was previously developed to predict the electrophoretic mobilities of DNA−RNA hybrids of the first-generation DQAMmiR.[27] Here we adapted this model to PNA−RNA hybrids of the second-generation DQAMmiR. The theoretical results indicated that the PNA−RNA hybrids with different numbers of base pairs could be separated from each other without drag tags, while the peptide drag tags on the PNA probes would still be useful mobility shifters for PNA−RNA hybrids of the same length. The proposed model suggested that using PNA probes in DQAMmiR would simplify the assay via two ways: by making SSB unnecessary and by decreasing the number of probes conjugated with drag tags. The basic schematic of the second-generation DQAMmiR with PNA hybridization probes is shown in Figure 1. We proved the feasibility of PNA-facilitated DQAMmiR by analyzing three

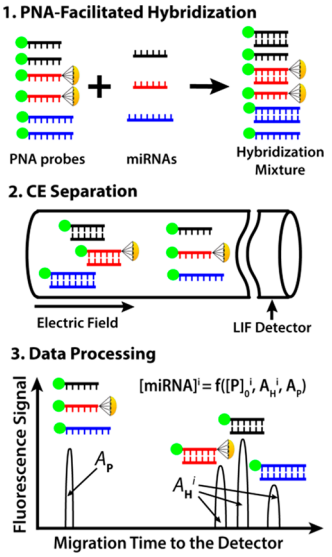

Figure 1. Schematic depiction of DQAMmiR with PNA hybridization probes.

miRNAs (miR-21, miR147a, and miR-378g), which have 20, 20, and 22 nucleotides, respectively. High accuracy and precision along with low LOQ indicate that DQAMmiR with PNA hybridization probes may potentially serve as a tool for practical miRNA analyses in clinical samples.

MATERIALS AND METHODS

MiRNAs and PNA Probes. All miRNAs were custom-synthesized by IDT (Coralville, IA, USA). All PNA probes were custom-synthesized by PNA Bio (Thousand Oak, CA, USA). Detailed information on miRNAs and PNA probes can be found in the Supporting Information. Concentrations of miRNA and PNA probes in stock solutions were determined using light absorbance at 260 nm measured with a NanoDrop ND-1000 spectrophotometer (Thermo-Fisher Scientific, Waltham, MA, USA); the extinction coefficients were provided by respective suppliers of miRNA and PNA. Acetonitrile (20%, v/v) was added to all buffers to improve PNA solubility.

Hybridization Reactions. Hybridization was carried out in a Mastercycler 5332 thermocycler (Eppendorf, Hamburg, Germany). Various concentrations of three miRNAs were incubated with 10 nM of their respective PNA probes in the CE running buffer (20 mM Borax, 120 mM NaCl, 20% acetonitrile, pH 9.0). According to the information provided by the supplier of PNA, all the PNA−miRNA hybrids used in this study have a melting temperature (T_m) above 80 °C. Thus, we selected 60 °C as the hybridization temperature, which is about 20 °C lower than their T_m and favorable for the hybridization reactions.[28] The temperature was first increased to a denaturing level of 95 °C and then lowered to 60 °C at a rate of 20 °C/min. After that, the temperature was held at 60 °C for 30 min to allow hybridization. To minimize RNA degradation, a nuclease-free environment was maintained while handling miRNA samples.

Capillary Electrophoresis. All experiments were performed using a P/ACE MDQ CE instrument (SCIEX, Brea, CA, USA) equipped with a laser-induced fluorescence detector. We used bare fused-silica capillaries with an outer diameter of 365 μm, an inner diameter of 50 μm, and a total length of 80 cm. The distance from the injection end of the

DOI: 10.1021/acs.analchem.8b04793
Anal. Chem. 2018, 90, 14610−14615

capillary to the detector was 70 cm. The capillary was flushed prior to every CE run with methanol, 0.1 M HCl, 0.3 M NaOH, deionized H_2O, and the running buffer for 1 min each under a 20 psi pressure. The sample was injected into the capillary by a 5 s pressure pulse of 0.5 psi. Electrophoresis was driven by an electric field of 312.5 V/cm with positive polarity at the capillary inlet. The capillary coolant temperature was kept at 20 °C during CE experiments. Fluorescence of the Alexa488 label on the PNA probes was excited by 488 nm light generated with a continuous-wave solid state laser (JDSU, Milpitas, CA, USA). Electropherograms were analyzed with 32 Karat Software. Peak areas were divided by the corresponding migration times to compensate for the dependence of the residence time in the detector on the electrophoretic velocity of the analyte. The quantity of each miRNA was calculated using these peak areas (see the Supporting Information for details).

RESULTS AND DISCUSSION

In DQAMmiR, accurate quantitation of multiple miRNAs relies on the separation of the nonhybridized probes from the miRNA-probe hybrids and hybrids from each other by CE. To establish DQAMmiR with PNA probes, it is necessary to investigate the separation of the PNA probe from the PNA−miRNA hybrid. A proof-of-principle experiment was performed using miR-21 and its complementary PNA probe. The result confirmed that the negatively charged PNA−RNA hybrid was separable from the excess of the neutral PNA probe without any mobility shifter (Figure 2). A near 10 min time window

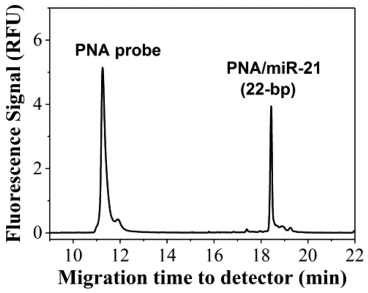

Figure 2. CE separation of a PNA probe from a PNA-miR-21 hybrid in a running buffer of 20 mM Borax and 20% acetonitrile at pH 9.0. The sample was prepared by incubating 2 nM miR-21 with a 10 nM PNA probe with a sequence fully complementary to miR-21. Separation was driven by an electric field of 312.5 V/cm at 20 °C.

was obtained between the PNA probe and the PNA−miRNA hybrid, which would allow theoretical separation of up to 30 hybrids (Supporting Information). The observed quality of separation of the excess PNA probe from the hybrid suggests that this PNA-facilitated assay could analyze miRNAs with high multiplexing capacity.

Another essential step for PNA-facilitated DQAMmiR was to separate PNA−miRNA hybrids from each other. For this purpose, theoretical estimates of the electrophoretic mobility of PNA−RNA hybrids were found by adapting to these hybrids a theoretical model previously developed for DNA−RNA hybrids.[27] In that model, the DNA−RNA duplex was assumed to behave like a rigid rod, because the contour lengths $L_{hyb} = N_{hyb}b$ (N_{hyb} is the number of base pairs, and b is the helical rise per base) for such short hybrids (18−25 bp) are shorter than their Kuhn length b_K. For the case of PNA−RNA duplexes, b = 0.24 nm leads to 4.32 nm ≤ L_{hyb} ≤ 6 nm (since 18 ≤ N_{hyb} ≤ 25),[29] while the Kuhn length of these helices can be estimated to be larger than 60 nm (b_K > 60 nm) (Supporting Information). Thus, the condition of $L_{hyb} << b_K$ is also satisfied in the case of PNA−RNA duplexes, and the rigid-rod model can be adapted to predict the mobilities of PNA−RNA hybrids. Thus, the expressions for the electric force ($F_{E,hyb}$) and hydrodynamic friction force ($F_{f,hyb}$) are[30,31]

$$F_{E,hyb} = \frac{eL_{hyb}}{z_i\lambda_B}E \tag{1}$$

$$F_{f,hyb} = 2\pi\eta L_{hyb}u_{rel}\left(\ln\frac{2L_{hyb}}{d_{hyb}} - 0.72\right)^{-1} \tag{2}$$

Here $L_{hyb} = N_{hyb}b$ is the length of the hybrid, and d_{hyb} is the diameter of the hybrid, which is approximately 3.5 nm for PNA−RNA duplexes.[29] z_i is the valence of the counterions. λ_B and η are the Bjerrum length and viscosity of the solution, which can be found to be 0.79 nm and 1.10 mPa·s, respectively, for the 20% (v/v) acetonitrile-containing aqueous solutions at 20 °C (Supporting Information). u_{rel} is the velocity of the hybrid with respect to the running buffer. Thus, the mobility of the PNA hybrid can be found from the balance of the electric force and the hydrodynamic friction force exerted on it.

$$F_{E,hyb} = F_{f,hyb} \tag{3}$$

Combining eqs 1−3, the expression for electrophoretic mobility μ_{hyb} can be written as

$$\mu_{hyb} = \frac{u_{rel}}{E} = \frac{e}{2\pi z_i\eta\lambda_B}\left(\ln\frac{2N_{hyb}b}{d_{hyb}} - 0.72\right) \tag{4}$$

Eq 4 suggests that the mobility of a PNA−RNA hybrid depends on the number of base pairs of the hybrid (N_{hyb}). Such a dependence was also found in our previous model of the DNA−RNA hybrids, although we neglected this effect and assumed for simplicity that different-length DNA−RNA hybrids had the same mobility.[27] This dependence is stronger for PNA−RNA hybrids because of the smaller value of b/d_{hyb} for the PNA−RNA helix (b = 0.24 nm, d_{hyb} = 3.5 nm) as compared with the DNA−RNA helix (b = 0.34 nm, d_{hyb} = 2.6 nm) (See Figure S1 in the Supporting Information).

The validity of this model was tested by theoretically estimating the electrophoretic mobility of PNA-miR-21 (N_{hyb} = 22) and comparing it with the experimentally measured value. The electrophoretic mobility of the PNA-miR-21 hybrid was calculated to be 1.12 × 10^{-4} $cm^2{\cdot}V^{-1}{\cdot}s^{-1}$, while the experimental result led to a value of 1.20 × 10^{-4} $cm^2{\cdot}V^{-1}{\cdot}s^{-1}$ (as shown in Figure 2). The small deviation of the calculated value from the experimental value suggested the model's applicability to PNA−RNA hybrids. Simulated electropherograms of PNA−RNA hybrids with different numbers of base pairs were obtained by using μ_{EOF} = 3.14 × 10^{-4} $cm^2{\cdot}V^{-1}{\cdot}s^{-1}$ (which corresponds to our running buffer containing 20 mM Borax and 20% acetonitrile at pH 9.0) as shown in Figure 3A. It is clear that a single-base-pair difference in lengths of PNA−RNA hybrids can cause significant difference in their electrophoretic mobilities. Such difference in mobilities should allow the separation of different-length PNA−miRNA hybrids from each other.

DOI: 10.1021/acs.analchem.8b04793
Anal. Chem. 2018, 90, 14610−14615

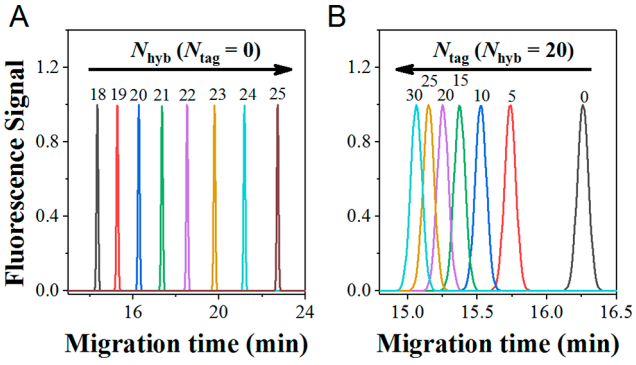

Figure 3. Simulated electropherograms of different PNA−RNA hybrids. (A) PNA−RNA hybrids with numbers of base pairs (N_{hyb}) in a range of 18−25. (B) PNA−RNA hybrids (20 bp) with lengths (numbers of amino acids) of peptide tags (N_{tag}) in a range of 0−30. Migration times of peaks shown above were estimated by using μ_{EOF} = 3.14×10^{-4} $cm^2 \cdot V^{-1} \cdot s^{-1}$, which was experimentally measured for our CE running buffer containing 20 mM Borax and 20% (v/v) acetonitrile at pH 9.0.

On the other hand, molecules with similar mobility, such as different-sequence but same-length PNA−miRNA hybrids, can also be electrophoretically separated from each other by end-labeled free solution electrophoresis (ELFSE).[32] By using this approach, we have developed universal peptide drag tags conjugated on the ssDNA probes as mobility shifters to separate ssDNA−miRNA hybrids in our first-generation DQAMmiR.[25] In this case, these peptide drag tags could also be applied to facilitate separation of different-sequence but same-length PNA−miRNA hybrids. For this purpose, we also estimated the electrophoretic mobility of PNA−RNA hybrids conjugated with different-length peptide drag tags. When the hydrodynamic friction force acting on the drag tag ($F_{f,tag}$) is taken into account, eq 3 can be rewritten as

$$F_{E,hyb} = F_{f,hyb} + F_{f,tag} \quad (5)$$

The hydrodynamic force, $F_{f,tag}$, acting upon the drag tag can be described via the expression

$$F_{f,tag} = 6\pi\eta R_{H,tag} u_{rel} \quad (6)$$

where $R_{H,tag}$ is the hydrodynamic radius of the drag tag. By substituting eqs 1, 2, and 6 for $F_{E,hyb}$, $F_{f,hyb}$, and $F_{f,tag}$, respectively, into 5 and by solving the resulting equation, we can obtain the expression for electrophoretic mobility of PNA−RNA hybrids with peptide drag tags

$$\mu_{hyb+tag} = \frac{e}{2\pi z_i \eta \lambda_B}\left[\left(\ln\frac{2N_{hyb}b}{d_{hyb}} - 0.72\right)^{-1} + \frac{3R_{H,tag}}{N_{hyb}b}\right]^{-1} \quad (7)$$

Studies of unfolded peptides have resulted in the following dependence for the hydrodynamic radius $R_{H,tag}$ (in nm) of short peptides by fitting empirical data[33]

$$R_{H,tag} = (0.22 \pm 0.11)N_{tag}^{0.57\pm0.02} \quad (8)$$

Here, N_{tag} is the number of amino-acid residues in the peptide chain. The hydrodynamic radii of peptide drag tags with different numbers of amino-acid residues can be estimated using eq 8. Thus, mobilities of PNA−RNA hybrids with different-length peptide drag tags could be estimated. As an example, the simulated electropherograms of 20-bp PNA−RNA hybrids with different-length peptide drag tags conjugated on the probe are shown in Figure 3B. The estimated electrophoretic mobilities of different PNA−miRNA hybrids can be found in the Supporting Information, indicating that the PNA−miRNA hybrids could be separated from each other by either the difference in numbers of nucleotides or lengths of peptide drag tags. The simulation strongly suggests that using PNA probes can simplify DQAMmiR by reducing the need for conjugation of drag tags.

As proof-of-principle, three miRNA targets, miR-147a, miR-378g, and miR-21, which have the numbers of nucleotides of 20, 20, and 22, respectively, were analyzed by DQAMmiR with PNA hybridization probes. Two PNA probes complementary to miR-378g and miR-21 were custom-synthesized without drag tags, while a PNA probe complementary to miR-147a was conjugated with a five-amino-acid tag.

We first performed CE separation with a running buffer of 20 mM Borax and 20% acetonitrile at pH 9.0 (Figure 4A). As a result, the 22-bp PNA−miRNA-21 hybrid exhibited the highest electrophoretic mobility, while the PNA-miR-147a (20 bp, 5 aa) was found to have the lowest electrophoretic mobility, which agreed well with our theoretical predictions. While deviations of 29, 24, and 6% were found between the theoretically predicted mobilities of PNA-miR-147a (20 bp, 5 aa), PNA-miR-378g (20 bp), and PNA-miR-21 (22 bp) and their respective experimentally measured mobilities, the qualitative agreement between the theoretical prediction and experimental results was evident: (i) the electrophoretic mobility of the PNA−miRNA hybrid depended on the number of base pairs in the hybrid, and the shorter hybrid had the lower electrophoretic mobility; (ii) the mobility of the hybrid could be altered by conjugating with a peptide drag tag on the PNA probe. However, a mobility shift by the 5-aa peptide tag on the PNA-miR-147a hybrid was not sufficient for baseline separation of the two 20-bp hybrids (baseline separation is preferable for high accuracy of miRNA quantitation). The resolution in CE separation can be improved by suppressing the EOF of the running buffer,[34] which can be achieved, in particular, by increasing the ionic strength of CE running buffer. Here, we added 120 mM NaCl into the running buffer

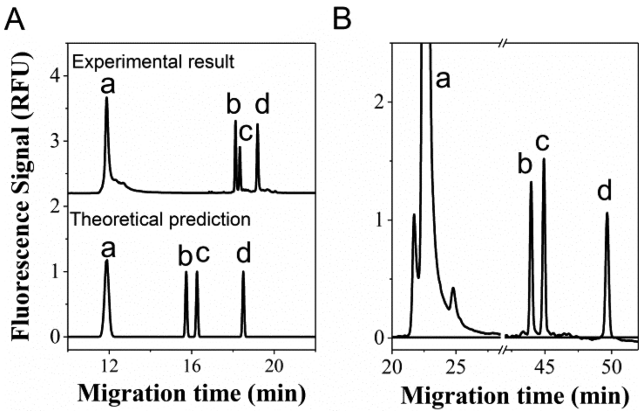

Figure 4. (A) Comparison of experimental and predicted separations of three PNA−miRNA hybrids in 20 mM Borax and 20% acetonitrile at pH 9.0. (B) Baseline separation of the three hybrids from each other by using a high-ionic-strength CE running buffer: 20 mM Borax, 120 mM NaCl, 20% acetonitrile, pH 9.0. Peak assignment: (a) excess PNA probes, (b) PNA-miR-147a (20 bp, 5 aa), (c) PNA-miR-378g (20 bp), and (d) PNA-miR-21 (22 bp).

DOI: 10.1021/acs.analchem.8b04793
Anal. Chem. 2018, 90, 14610−14615

to suppress EOF and prolong separation. As a result, baseline separation was achieved, leading to a peak resolution of 3.1 between PNA-miR-147a and PNA-miR-378g (Figure 4B). Thus, the running buffer for the following experiments was 20 mM Borax, 120 mM NaCl and 20% acetonitrile at pH 9.0.

To study the suitability of PNA-facilitated DQAMmiR for miRNA quantitation, measurements of miR-147a, miR-378g, and miR-21 were performed simultaneously in a concentration range of 32−500 pM, which is of interest for analyzing miRNAs in clinical samples.[22] In all experiments, final concentrations of all three PNA probes in hybridization mixtures were set at 10 nM, which is an excess to all targets. The electropherograms obtained in these experiments are shown in Figure 5A. Concentrations of individual miRNAs

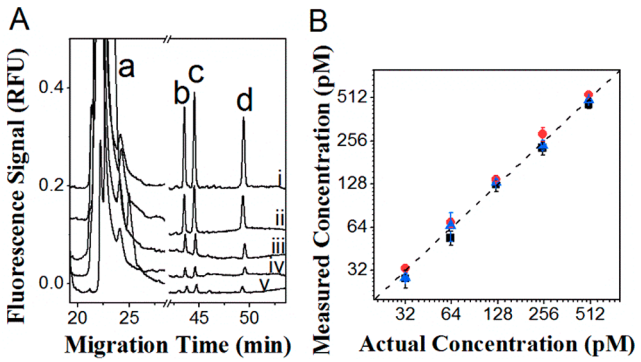

Figure 5. (A) Electropherograms of PNA-facilitated measurements. Peak assignment: (a) excess PNA probes, (b) PNA-miR-147a (20 bp, 5 aa), (c) PNA-miR-378g (20 bp), (d) PNA-miR-21 (22 bp). Electropherograms i−vi correspond to target concentrations of 500, 250, 125, 63, and 32 pM, respectively. B) Quantitation of three miRNAs simultaneously by PNA-facilitated DQAMmiR. Concentrations measured with DQAMmiR are shown with respect to their actual values determined by light absorbance at 260 nm. miR-21, miR-147a, and miR-378g are represented by black rectangles, red circles, and blue triangles, respectively. The dashed line ($y = x$) represents a line corresponding to 100% recovery. Error bars show one standard deviation from mean values obtained from three experiments.

were calculated by using a math strategy developed in the previous DQAMmiR study (Supporting Information)[22]

$$[\text{miRNA}]^i = \frac{A_H^i}{q_H^i q_P^i} \frac{\sum_{i=1}^{N} (q_P^i [P]_0^i)}{A_P + \sum_{i=1}^{N} \frac{A_H^i}{q_H^i}} \quad (9)$$

$[P]_0^i$ is the total concentration of the i-th PNA probe (composed of the hybrid and the excess probe), A_H^i is the area corresponding to the i-th hybrid, A_P is the cumulative area of the unbound probes, q_P^i is a relative quantum yield of the i-th PNA probe to normalize the quantum yield differences between the probes, and q_H^i is the relative quantum yield of the i-th hybrid with respect to that of the unbound probe. Both q_P^i and q_H^i were determined in separate experiments (Supporting Information). Using eq 9, we were able to determine concentrations of the three targets simultaneously by quantitating peak areas from a single electropherogram without building/using a calibration curve.

The measured concentrations of the three targets were compared with their actual concentrations as shown in Figure 5B. A recovery of over 90% with RSD of approximately 10% was observed for measuring all three miRNAs with concentrations varying in a 32−500 pM range (Supporting Information). Also, by studying the signal-to-noise ratio (SNR) of the peaks of hybrids, the lower limit-of-quantitation (LOQ) of this method performed with a commercial CE-LIF instrument was determined to be 14 pM. These results demonstrate that this PNA-facilitated DQAMmiR is capable of quantitating multiple miRNAs with high accuracy and precision at picomolar concentrations.

In contrast to DNA probes, PNA probes have greater specificity in hybridizing with DNA or RNA, with a PNA−DNA base mismatch being more destabilizing than a similar mismatch in a DNA−DNA duplex.[35] This property will allow us to establish PNA-facilitated DQAMmiR for analyzing miRNAs with slightly different sequences by simply changing conditions of the hybridization reaction, such as temperature, addition of denaturing reagent, and etc. PNAs are also resistant to degradation by nucleases or proteases,[36] making them perfect hybridization probes for analysis of miRNAs in biological samples. As a result, PNA-facilitated DQAMmiR can be potentially a practical tool for quantitation of miRNAs in clinical samples.

CONCLUSIONS

In this study, we introduced the second-generation DQAMmiR, which utilizes electrically neutral PNA probes instead of negatively charged DNA probes. In this approach, the negatively charged PNA−miRNA hybrids were separated from the neutral PNA probes by CE without any additional mobility shifter, leading to a near 10 min time window, which would allow us to analyze up to 30 miRNAs simultaneously. The theoretical study of the electrophoretic mobility of PNA−miRNA hybrid qualitatively predicted that the separation of the hybrids from each other could be achieved by utilizing their differences in either (i) the number of base pairs or (ii) the length of peptide drag tags. This was confirmed by our experimental results. Our proof-of-principle study demonstrated that PNA-facilitated DQAMmiR was able to quantify three miRNAs simultaneously with high accuracy (recovery > 90%) and precision (RSD ≈ 10%) with a LOQ of 14 pM by using a commercial CE instrument, suggesting that DQAMmiR with PNA hybridization probes may facilitate validation and clinical use of miRNA biomarkers.

ASSOCIATED CONTENT

Supporting Information

The Supporting Information is available free of charge on the ACS Publications website at DOI: 10.1021/acs.analchem.8b04793.

Sequences of miRNA targets and their PNA probes; estimation of the multiplexing capacity in the separation window; assumption of the short PNA−miRNA hybrid behaving as a rigid rod; the Bjerrum length (λ_B) and viscosity (η) of the 20% (v/v) containing solutions; dependence of the relative mobility of a hybrid on the number of base pairs of the hybrid; theoretical estimated electrophoretic mobilities of PNA−miRNA hybrids; simulated electropherograms of the PNA−miRNA hybrids; relative quantum yield measurements; derivation of equations for the determination of concentrations of multiple miRNA by PNA-facilitated DQAMmiR; quantitation results of PNA-facilitated DQAMmiR (PDF)

DOI: 10.1021/acs.analchem.8b04793
Anal. Chem. 2018, 90, 14610−14615

AUTHOR INFORMATION

Corresponding Author

*E-mail: skrylov@yorku.ca.

ORCID

Liang Hu: 0000-0003-4507-8525
Svetlana M. Krylova: 0000-0002-3291-6721
Burton B. Yang: 0000-0002-2892-7209
Stanley K. Liu: 0000-0001-6851-0857
George M. Yousef: 0000-0003-3859-779X
Sergey N. Krylov: 0000-0003-3270-2130

Author Contributions

Liang Hu and Mansi Anand contributed equally to this manuscript. The manuscript was written through contributions of all authors. All authors have given approval to the final version of the manuscript.

Notes

The authors declare no competing financial interest.

ACKNOWLEDGMENTS

We thank Canadian Institutes of Health Research (grant number CPG 134747) and the Natural Sciences and Engineering Research Council of Canada (grant number CHRP 462341-2014) for financial support.

REFERENCES

(1) He, L.; Hannon, G. J. *Nat. Rev. Genet.* **2004**, *5*, 522−531.
(2) Tüfekci, K. U.; Meuwissen, R. L. J.; Genç, Ş. In *miRNomics: MicroRNA Biology and Computational Analysis*; Yousef, M., Allmer, J., Eds.; Humana Press: Totowa, NJ, 2014; pp 15−31.
(3) Femminella, G. D.; Ferrara, N.; Rengo, G. *Front. Physiol.* **2015**, *6*, 40.
(4) Catalucci, D.; Latronico, M. V.; Condorelli, G. *Ann. N. Y. Acad. Sci.* **2008**, *1123*, 20−29.
(5) Romero-Cordoba, S. L.; Salido-Guadarrama, I.; Rodriguez-Dorantes, M.; Hidalgo-Miranda, A. *Cancer Biol. Ther.* **2014**, *15*, 1444−1455.
(6) Brase, J. C.; Johannes, M.; Schlomm, T.; Falth, M.; Haese, A.; Steuber, T.; Beissbarth, T.; Kuner, R.; Sultmann, H. *Int. J. Cancer* **2011**, *128*, 608−616.
(7) Zheng, D.; Haddadin, S.; Wang, Y.; Gu, L.-Q.; Perry, M. C.; Freter, C. E.; Wang, M. X. *Int. J. Clin. Exp. Pathol.* **2011**, *4*, 575−586.
(8) van Schooneveld, E.; Wouters, M. C.; Van der Auwera, I.; Peeters, D. J.; Wildiers, H.; Van Dam, P. A.; Vergote, I.; Vermeulen, P. B.; Dirix, L. Y.; Van Laere, S. *Breast Cancer Res.* **2012**, *14*, R34.
(9) Pritchard, C. C.; Cheng, H. H.; Tewari, M. *Nat. Rev. Genet.* **2012**, *13*, 358.
(10) Wang, B.; Howel, P.; Bruheim, S.; Ju, J.; Owen, L. B.; Fodstad, O.; Xi, Y. *PLoS One* **2011**, *6*, e17167.
(11) de Bang, T. C.; Shah, P.; Cho, S. K.; Yang, S. W.; Husted, S. *Anal. Chem.* **2014**, *86*, 6823−6826.
(12) Xu, F.; Zhou, W.; Cao, J.; Xu, Q.; Jiang, D.; Chen, Y. *Theranostics* **2017**, *7*, 2849−2862.
(13) Labib, M.; Khan, N.; Ghobadloo, S. M.; Cheng, J.; Pezacki, J. P.; Berezovski, M. V. *J. Am. Chem. Soc.* **2013**, *135*, 3027−3038.
(14) Yang, C.; Dou, B.; Shi, K.; Chai, Y.; Xiang, Y.; Yuan, R. *Anal. Chem.* **2014**, *86*, 11913−11918.
(15) Qavi, A. J.; Bailey, R. C. *Angew. Chem., Int. Ed.* **2010**, *49*, 4608−4611.
(16) Yin, B.-C.; Liu, Y.-Q.; Ye, B.-C. *J. Am. Chem. Soc.* **2012**, *134*, 5064−5067.
(17) Lee, H.; Shapiro, S. J.; Chapin, S. C.; Doyle, P. S. *Anal. Chem.* **2016**, *88*, 3075−3081.
(18) Roy, S.; Soh, J. H.; Gao, Z. *Lab Chip* **2011**, *11*, 1886−1894.
(19) Cheng, Y.; Dong, L.; Zhang, J.; Zhao, Y.; Li, Z. *Analyst* **2018**, *143*, 1758−1774.
(20) Mraz, M.; Malinova, K.; Mayer, J.; Pospisilova, S. *Biochem. Biophys. Res. Commun.* **2009**, *390*, 1−4.
(21) Nagy, Z. B.; Wichmann, B.; Kalmar, A.; Bartak, B. K.; Tulassay, Z.; Molnar, B. *Pathol. Oncol. Res.* **2016**, *22*, 505−513.
(22) Wegman, D. W.; Krylov, S. N. *Angew. Chem., Int. Ed.* **2011**, *50*, 10335−10339.
(23) Hu, L.; Stasheuski, A. S.; Wegman, D. W.; Wu, N.; Yang, B. B.; Hayder, H.; Peng, C.; Liu, S. K.; Yousef, G. M.; Krylov, S. N. *Anal. Chem.* **2017**, *89*, 4743−4748.
(24) Krylova, S. M.; Wegman, D. W.; Krylov, S. N. *Anal. Chem.* **2010**, *82*, 4428−4433.
(25) Wegman, D. W.; Cherney, L. T.; Yousef, G. M.; Krylov, S. N. *Anal. Chem.* **2013**, *85*, 6518−6523.
(26) Egholm, M.; Buchardt, O.; Nielsen, P. E.; Berg, R. H. *J. Am. Chem. Soc.* **1992**, *114*, 1895−1897.
(27) Cherney, L. T.; Krylov, S. N. *Analyst* **2013**, *138*, 553−558.
(28) Weiler, J.; Gausepohl, H.; Hauser, N.; Jensen, O. N.; Hoheisel, J. D. *Nucleic Acids Res.* **1997**, *25*, 2792−2799.
(29) Kiliszek, A.; Banaszak, K.; Dauter, Z.; Rypniewski, W. *Nucleic Acids Res.* **2016**, *44*, 1937−1943.
(30) Manning, G. S. *J. Chem. Phys.* **1969**, *51*, 924−933.
(31) Happel, J.; Brenner, H. *Low Reynolds number hydrodynamics: with special applications to particulate media*; Springer Netherlands: Dordrecht, 1983; pp 159−234.
(32) Heller, C.; Slater, G. W.; Mayer, P.; Dovichi, N.; Pinto, D.; Viovy, J.-L.; Drouin, G. *J. Chromatogr. A* **1998**, *806*, 113−121.
(33) Wilkins, D. K.; Grimshaw, S. B.; Receveur, V.; Dobson, C. M.; Jones, J. A.; Smith, L. J. *Biochemistry* **1999**, *38*, 16424−16431.
(34) Kaneta, T.; Tanaka, S.; Yoshida, H. *J. Chromatogr. A* **1991**, *538*, 385−391.
(35) Nielsen, P. E. *Annu. Rev. Biophys. Biomol. Struct.* **1995**, *24*, 167−183.
(36) Demidov, V. V.; Potaman, V. N.; Frank-Kamenetskil, M. D.; Egholm, M.; Buchard, O.; Sonnichsen, S. H.; Nlelsen, P. E. *Biochem. Pharmacol.* **1994**, *48*, 1310−1313.

DOI: 10.1021/acs.analchem.8b04793
Anal. Chem. 2018, 90, 14610−14615